Learning from a Mineral Structure toward an Ultra-Narrow-Band Blue-Emitting Silicate Phosphor $RbNa_3(Li_3SiO_4)_4$:Eu^{2+}

Hongxu Liao[+], Ming Zhao[+], Maxim S. Molokeev, Quanlin Liu, and Zhiguo Xia*

Abstract: Learning from natural mineral structures is an efficient way to develop potential host lattices for applications in phosphor converted (pc)LEDs. A narrow-band blue-emitting silicate phosphor, $RbNa_3(Li_3SiO_4)_4$:Eu^{2+} (RNLSO:Eu^{2+}), was derived from the UCr_4C_4-type mineral model. The broad excitation spectrum (320–440 nm) indicates this phosphor can be well matched with the near ultraviolet (n-UV) LED chip. Owing to the UCr_4C_4-type highly condensed and rigid framework, RNLSO:Eu^{2+} exhibits an extremely small Stokes shift and an unprecedented ultra-narrow (full-width at half-maximum, FWHM = 22.4 nm) blue emission band ($\lambda_{em} = 471$ nm) as well as excellent thermal stability (96 %@150°C of the initial integrated intensity at 25°C). The color gamut of the as-fabricated (pc)LEDs is 75 % NTSC for the application in liquid crystal displays from the prototype design of an n-UV LED chip and the narrow-band RNLSO:Eu^{2+} (blue), β-SiAlON:Eu^{2+} (green), and K_2SiF_6:Mn^{4+} (red) components as RGB emitters.

Phosphor-converted white light-emitting diodes (pc-wLEDs) are considered for emerging backlight units in modern liquid-crystal display (LCD) applications, which mainly focused on improvements of resolution and power consumption over the past few years.[1] The improvement of the color gamut, however, has becomes a hot issue. Color gamut is determined by the color coordinates of red, green, and blue (RGB) emissions emitted from white LEDs passing through the corresponding RGB color filters. Compared to those utilizing the combination of individual RGB LED chips, pc-wLEDs are more reliable and simple.[2] Therefore, the

luminescent properties (for example, peak emission wavelength and full-width at half-maximum (FWHM)) of phosphors used directly affect the space of the color gamut.[3] Accordingly, the development of narrow-emitting phosphors in the RGB spectral region has been a tremendous challenge, which further required a specific peak position, high quantum efficiency, and excellent thermal stability.[4] Recently, several types of red and green emitting phosphors for backlights have been reported. Moreover, quantum dots (QDs) emitters have also demonstrated significant advantages for LCD backlights; however, the poor chemical and thermal stability restrict their applications.[5] By far, β-SiAlON:Eu^{2+} and K_2SiF_6:Mn^{4+} (KSF:Mn^{4+}) are accepted as the most promising green and red phosphors, respectively, for wide color gamut wLEDs backlights.

To date, the discovery of the narrow-band phosphors has drawn much attention from the consideration of both academic researches and industrial investigations. From a viewpoint of materials design, narrow-band phosphors can be achieved by a rigid host lattice providing a highly symmetric dopant site (for example, Eu^{2+}, Ce^{3+}) with a high coordination number.[6] For example, the recently reported narrow-band red-emitting $Sr[LiAl_3N_4]$:Eu^{2+} phosphor by Schnick et al., which belongs to the UCr_4C_4-type prototype structure, provides an efficient thought of exploring phosphor, the highly condensed structure and rigid framework leading to the narrow-band emission.[7] Moreover, Schnick's group recently reported the narrow cyan-emitting Eu^{2+}-doped oxonitridoberyllate phosphor, $SrBe_6ON_4$:Eu^{2+} ($\lambda_{em} = 495$ nm; FWHM = 35 nm), and the narrow-band character is originated from the highly condensed structure with a 3D network of $BeON_3$ and BeN_4 tetrahedra.[8] They also just discovered the ultra-narrow band blue-emitting oxoberyllates $AELi_2[Be_4O_6]$:Eu^{2+} (AE = Sr, Ba) exhibiting a rigid covalent network isotypic to the nitridoalumosilicate $BaLi_2[(Al_2Si_2)N_6]$:Eu^{2+}.[4a] Reviewing the above-mentioned narrow-band phosphors, the rigid network is the base for the narrow-band emission, as it limits the local structural relaxation of the dopant (Eu^{2+}) site in its excited state and allows a small Stokes-shift.[4a] Recently, our group conducted the work from natural mineral learning and proposed the mineral-inspired prototype evolution and new phase construction strategy, and it is proved to be efficient for the discovery of the potential host lattices for application in phosphor converted (pc)LEDs.[9] To design the new narrow-band phosphors, developing UCr_4C_4-type structure phosphor may find chances for tunable or improved properties. However, previous researches mainly focus on nitrides, the oxide-based UCr_4C_4-type phosphor was seldom investigated. Herein, we designed and prepared a new oxide-based

[*] H. X. Liao,[+] M. Zhao,[+] Prof. Dr. Q. L. Liu, Prof. Dr. Z. G. Xia
The Beijing Municipal Key Laboratory of New Energy Materials and Technologies, School of Materials Sciences and Engineering
University of Science and Technology Beijing
Beijing 100083 (P. R. China)
E-mail: xiazg@ustb.edu.cn

Prof. Dr. M. S. Molokeev
Laboratory of Crystal Physics, Kirensky Institute of Physics
Federal Research Center KSC SB RAS
Krasnoyarsk 660036 (Russia)
and
Siberian Federal University
Krasnoyarsk, 660041 (Russia)
and
Department of Physics, Far Eastern State Transport University
Khabarovsk, 680021 (Russia)

[+] These authors contributed equally to this work.

Supporting information and the ORCID identification number(s) for the author(s) of this article can be found under:
https://doi.org/10.1002/anie.201807087.

UCr$_4$C$_4$-type RbNa$_3$(Li$_3$SiO$_4$)$_4$:Eu^{2+} (RNLSO:Eu^{2+}) phosphor, which exhibits a narrow-band blue emission with FWHM of only 22.4 nm. The thermal quenching behavior and the optical property of the wLED were studied. The results suggest that RNLSO:Eu^{2+} phosphor can be a potential blue-emitting candidate for application in LCD technology from the prototype design of an nUV LED chip with the narrow-band green and red components.

Mineral learning focused on the crystal structure design plays an important role in the discovery of new LED phosphors, and it also opens up new avenues for the reconstruction of new phases via materials design. Clearly, this mineral-inspired strategy is based on the initial prototype compounds. As can be seen from Figure 1 a, the structure of
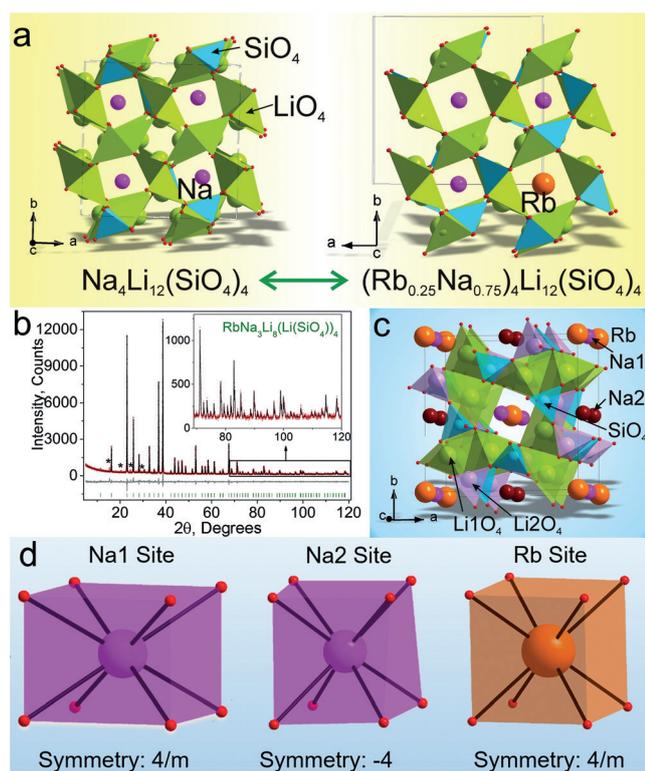

Figure 1. a) Mineral prototype inspired materials design from NaLi$_3$SiO$_4$ to RbNa$_3$(Li$_3$SiO$_4$)$_4$. b) The Rietveld refinement XRD pattern of RNLSO, and the minor unidentified phases marked by asterisks. c) Crystal structure of RNLSO. d) Coordination polyhedron of Na1, Na2, and Rb sites.

RbNa$_3$(Li$_3$SiO$_4$)$_4$ (RNLSO) originates from that of NaLi$_3$SiO$_4$, sharing the same UCr$_4$C$_4$-type model, and we can treat the former as one Na atom in RbNa$_3$(Li$_3$SiO$_4$)$_4$ is replaced by a Rb atom to correlate their structural similarity. Powder X-ray diffraction of as-prepared sample proves that the synthesis of RNLSO is successful (Supporting Information, Figure S1). The Rietveld refinement is shown in Figure 1 b, almost all peaks, besides small amount of tiny unknown impurity peaks marked by asterisks, were indexed by tetragonal cell (*I*4/*m*) with parameters close to RbNa$_3$-(Li$_3$SiO$_4$)$_4$.[10] Therefore, this crystal structure can be taken as

starting model for Rietveld refinement. Detailed information on the refinement processing (Supporting Information, Table S1) and the crystallographic information file (CIF) of this phase RbNa$_3$(Li$_3$SiO$_4$)$_4$ are provided in the Supporting Information. Coordinates of atoms and main bond lengths are also shown in the Supporting Information, Tables S2, S3. Figure 1 c shows the crystal structure of RNLSO highlighting three different cation sites, Rb, Na1, and Na2, which formed by a three-dimensional network of (Li/Si)O$_4$-tetrahedra. The framework is built by connecting edge-sharing and corner-sharing tetrahedra to each other, and Na/Rb atoms are filled in the ring channels. The degree of condensation (that is, the atom ratio (Li/Si):O) in RNLSO is $\kappa = 1$, illustrating the framework of this compound is highly condensed and rigid. To describe the local structure of cations, Na (Na1, Na2) and Rb coordination polyhedrons are provided in Figure 1 d, respectively. Na1 and Rb coordinated with eight O atoms in highly symmetric cuboid-like environment, but Na2 site, different with the above sites, has low symmetric environment. Anyway, high site symmetry, for example, cuboidal coordination, is considered as being favorable for a small Stokes shift, and thus a narrower emission band.

The ^{7}Li solid-state nuclear magnetic resonance (NMR) spectrum is shown in Figure 2 a. The chemical shift value of 4.524 ppm indicates that Li incorporates in the build of rigid
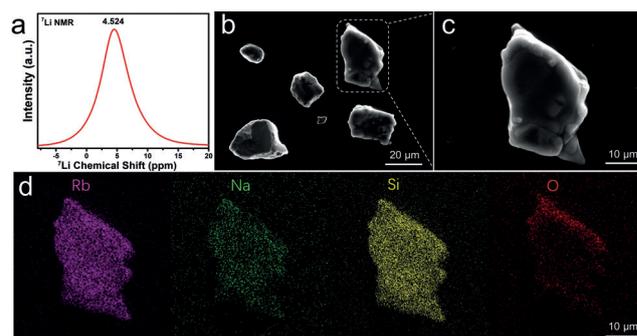

Figure 2. a) The ^{7}Li solid-state NMR spectrum of RNLSO:Eu^{2+}. b) Scanning electron microscope (SEM) images of RNLSO:Eu^{2+} crystal particles and c) enlarged particle. d) Element mapping images of Rb, Na, Si, and O for the chosen RNLSO:Eu^{2+} particle.

framework, and the only one broad-band signal is attributed to the similar two Li sites (Li1O$_4$ and Li2O$_4$) and the limited resolution of ^{7}Li.[7] To further exhibit the morphological features of RNLSO:Eu^{2+} particles, the scanning electron microscope (SEM) was conducted. The chosen particle size is about 20–30 μm, suggesting that the as-prepared RNLSO:Eu^{2+} sample is well crystallized (Figure 2 b,c). The energy-dispersive X-ray spectroscopy (EDS) and elemental mapping were performed to confirm the elemental composition and uniformity of RNLSO:Eu^{2+}. The average atomic ratio Rb/Na/Si/O of 0.97:3:4.9:16.2 determined by EDS (see details in the Supporting Information, Table S4) is close to the formula RbNa$_3$Li$_{12}$Si$_4$O$_{16}$, and the elemental mapping images (Figure 2 d) also indicate the uniform distribution of Rb, Na, Si, O in the phosphor particle.

As discussed above, the highly condensed network structure of RNLSO shows extraordinary effects on the luminescence properties. The photoluminescence emission (PL) and excitation (PLE) spectra of 3% Eu^{2+} doped RNLSO phosphor are shown in Figure 3a. RNLSO:Eu^{2+} exhibits two
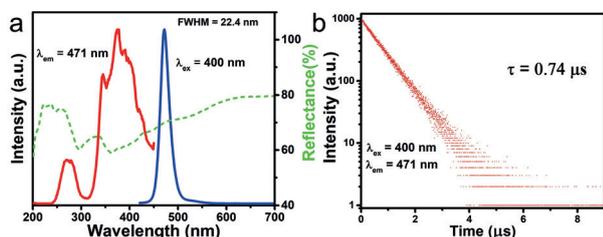

Figure 3. a) PL, PLE, and UV/vis spectra of blue-emitting RNLSO:Eu^{2+} (excitation = red line, emission = blue line, reflectance = green dashed line). b) The decay curve monitored at 471 nm of RNLSO:Eu^{2+} under excitation at 400 nm.

excitation bands from 250–300 nm and 320–440 nm, respectively, corresponding to the typical 4f–5d transitions of Eu^{2+},[7] which is also verified by a broad absorption band ranging from the UV to the blue spectral area. More importantly, the RNLSO:Eu^{2+} phosphor shows an amazing narrow-band blue emission peaking at 471 nm with FWHM of only 22.4 nm (ca. 980 cm^{-1}) at room temperature, which is ascribed to the highly condensed network structure. Furthermore, we measured the PL spectrum at 80 K of RNLSO:Eu^{2+} (Supporting Information, Figure S2). The emission band can be well divided into three Gaussian peaks locating at 21 305 cm^{-1} (469.37 nm), 21 174 cm^{-1} (472.28 nm) and 20 840 cm^{-1} (479.85 nm), respectively, indicating the presence of three different Eu^{2+} emission centers, originated from three cation sites (Rb, Na1, and Na2) occupied by Eu^{2+}. Two unprecedented narrow peaks with FWHM of about 2.5/5.3 nm can be associated with Eu^{2+} at Rb and Na1 sites with the highly cubic symmetry sites (4/*m*) and the slightly wide emission band with FWHM of about 17 nm should be related with Na2 site with the distorting cubic site (−4) (Figure 1d).[4a]

Owing to the narrow band emission, the color purity of this phosphor is calculated to be 83.3%. Under 400 nm excitation, the room temperature internal and external quantum efficiency values of RNLSO:3% Eu^{2+} are determined to be 53% and 13%, respectively, and the measurement details are shown in the Supporting Information, Figure S2. The decay curve of RNLSO:Eu^{2+} monitored at 400 nm excitation and 471 nm emission is shown in Figure 3b, and it can be well fitted into a single-exponential function:[11]

$$I(t) = I_0 + A \exp(-t/\tau) \qquad (1)$$

where I(t) and I$_0$ are the luminescence intensity at time *t* and *t* ≫ *τ*, *A* is a constant, *τ* is the lifetime exponential component. The lifetime value of RNLSO:Eu^{2+} is 0.74 μs.

Thermal stability is one of the most important properties of inorganic phosphors for the application.[12] Hence, the temperature-dependent PL spectra of RNLSO:Eu^{2+} were collected from room temperature 25°C to 250°C. As shown in

Figure 4a, the peak (λ$_{em}$ = 471 nm) intensity decreased, and the inset also shows the slight blue-shift of the peak positions depending on increasing temperature. As a quantitative analysis, the integrated emission intensity and the peak (471 nm) intensity at 150°C drop only 4% and 20% (Fig-
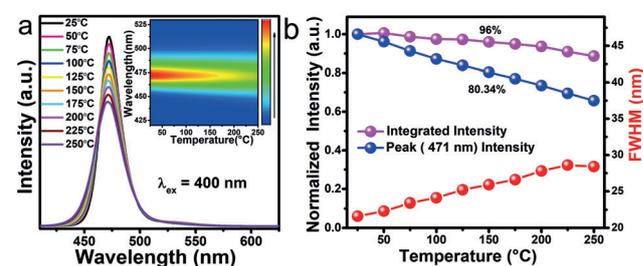

Figure 4. a) Thermal quenching behavior of PL spectra for RNLSO:Eu^{2+} phosphor under 400 nm excitation in the temperature range 25–250°C. Inset: the visual thermal quenching behavior. b) Temperature-dependent normalized integrated PL intensities and peak (471 nm) intensities of RNLSO:Eu^{2+}, as well as the variation of the FWHM depending on increasing temperature.

ure 4b) compared to the initial intensity at room temperature, and even at 250°C, the integrated emission intensity and the peak intensity are still about 88% and 66% of that in room temperature, indicating RNLSO:Eu^{2+} has an excellent thermal stability. The increasing temperature causes the change of FWHM (from 22.4 nm to 28 nm), which is the reason for the difference between integrated intensity and peak intensity; however, it still retains the unprecedented ultra-narrow blue emission.

Given the ultra-narrow band blue emission and excellent thermal stability of RNLSO:Eu^{2+}, it can be a good candidate for display backlights. To verify the suitability of RNLSO:Eu^{2+} as the blue component in the potential prototype design of n-UV LED chip with RGB emitters, the wLED was fabricated by using the title narrow-band phosphor including the commercial green phosphor β-SiAlON:Eu^{2+}, the commercial red phosphor KSF:Mn^{4+} and a n-UV LED chip (λ$_{em}$ = 395 nm). The emission spectrum of the fabricated wLED under a current of 40 mA as well as the as-fabricated and lightened white LED are provided in Figure 5a. The white LED provides a bright white light with a correlated color temperature (CCT) of 5064 K and the color render index (R$_a$) of 68.8. The CIE color coordinates of LED is (0.343 0.345), close to the standard white point at (0.33 0.33). Color space (Figure 5b) of the as-fabricated wLED can reach 75% of the National Television System Committee standard (NTSC), demonstrating potential application in LCD technology as an emerging realization strategy.

In summary, following the mineral-inspired prototype material design strategy, we developed a new blue-emitting oxide-based phosphor RbNa$_3$(Li$_3$SiO$_4$)$_4$:Eu^{2+} derived from the UCr$_4$C$_4$ prototype, which presents an unprecedented narrow band emission (λ$_{em}$ = 471 nm, FWHM = 22.4 nm) under 400 nm excitation comparable to well-known QDs emitter but with more stable properties. The integrated intensity at 150°C dropped only 4% compared to the initial
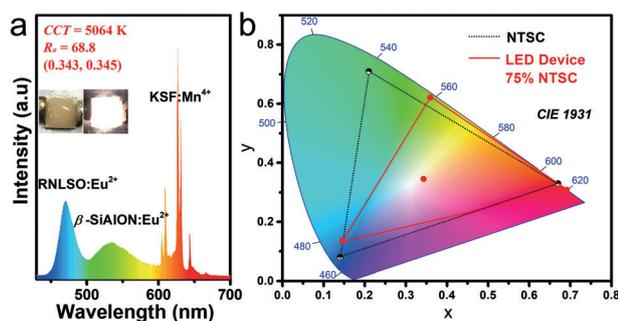
Figure 5. a) EL spectrum of the LED device fabricated with the blue phosphor RNLSO:Eu^{2+}, red phosphor KSF:Mn^{4+}, green phosphor β-SiAlON:Eu^{2+}, and a nUV chip ($\lambda_{em} = 395$ nm) under a current of 40 mA. Inset: photographs of as-fabricated and lightened white LED. b) CIE 1931 color coordinates of fabricated white LED, and color space of NTSC standard (short dotted line) and white LED device (red line).

intensity at room temperature. The highly condensed crystal structure contributes to the narrow band emission of RNLSO:Eu^{2+}. The wLED fabricated by coating the n-UV chip with the mixture of KSF:Mn^{4+} (red), β-SiAlON:Eu^{2+} (green), and RNLSO:Eu^{2+} (blue) phosphors can cover 75 % of the color space of NTSC, and the CCT and R_a value of the wLED are 5064 K and 68.8, respectively. RNLSO:Eu^{2+} phosphor with unique and extraordinary luminescence characteristics seems highly promising in emerging wLEDs application warrant further exploration.

Acknowledgements

Conflict of interest

The authors declare no conflict of interest.

[1] a) P. Pust, P. J. Schmidt, W. Schnick, *Nat. Mater.* **2015**, *14*, 454–458; b) Z. G. Xia, Q. L. Liu, *Prog. Mater. Sci.* **2016**, *84*, 59–117; c) B. Wang, H. Lin, F. Huang, J. Xu, H. Chen, Z. Lin, Y. Wang, *Chem. Mater.* **2016**, *28*, 3515–3524.

[2] R.-J. Xie, N. Hirosaki, T. Takeda, *Appl. Phys. Express* **2009**, *2*, 022401.

[3] a) J. S. Steckel, J. Ho, C. Hamilton, J. Xi, C. Breen, W. Liu, P. Allen, S. Coe-Sullivan, *J. Soc. Inf. Disp.* **2015**, *23*, 294–305; b) L. Wang, X. Wang, T. Kohsei, K. Yoshimura, M. Izumi, N. Hirosaki, R. J. Xie, *Opt. Express* **2015**, *23*, 28707–28717.

[4] a) P. Strobel, C. Maak, V. Weiler, P. J. Schmidt, W. Schnick, *Angew. Chem. Int. Ed.* **2018**, *57*, 8739–8743; *Angew. Chem.* **2018**, *130*, 8875–8879; b) A. C. Duke, S. Hariyani, J. Brgoch, *Chem. Mater.* **2018**, *30*, 2668–2675; c) S. Li, L. Wang, D. Tang, Y. Cho, X. Liu, X. Zhou, L. Lu, L. Zhang, T. Takeda, N. Hirosaki, R.-J. Xie, *Chem. Mater.* **2018**, *30*, 494–505; d) Y. Sato, H. Kato, M. Kobayashi, T. Masaki, D. H. Yoon, M. Kakihana, *Angew. Chem. Int. Ed.* **2014**, *53*, 7756–7759; *Angew. Chem.* **2014**, *126*, 7890–7893.

[5] L. Protesescu, S. Yakunin, M. I. Bodnarchuk, F. Krieg, R. Caputo, C. H. Hendon, R. X. Yang, A. Walsh, M. V. Kovalenko, *Nano Lett.* **2015**, *15*, 3692–3696.

[6] a) Z. G. Xia, A. Meijerink, *Chem. Soc. Rev.* **2017**, *46*, 275–299; b) J. H. Oh, Y. J. Eo, H. C. Yoon, Y.-D. Huh, Y. R. Do, *J. Mater. Chem. C* **2016**, *4*, 8326–8348.

[7] P. Pust, V. Weiler, C. Hecht, A. Tucks, A. S. Wochnik, A. K. Henss, D. Wiechert, C. Scheu, P. J. Schmidt, W. Schnick, *Nat. Mater.* **2014**, *13*, 891–896.

[8] P. Strobel, T. de Boer, V. Weiler, P. J. Schmidt, A. Moewes, W. Schnick, *Chem. Mater.* **2018**, *30*, 3122–3130.

[9] a) Z. G. Xia, K. R. Poeppelmeier, *Acc. Chem. Res.* **2017**, *50*, 1222–1230; b) Z. G. Xia, Z. Xu, M. Chen, Q. L. Liu, *Dalton Trans.* **2016**, *45*, 11214–11232.

[10] J. Hoffmann, R. Brandes, R. Hoppe, *Z. Anorg. Allg. Chem.* **1994**, *620*, 1495–1508.

[11] G. Blasse, B. Grabmaier, *Luminescent materials*, Springer, Heidelberg, **1994**, pp. 1–9.

[12] Y. H. Kim, P. Arunkumar, B. Y. Kim, S. Unithrattil, E. Kim, S. H. Moon, J. Y. Hyun, K. H. Kim, D. Lee, J. S. Lee, W. B. Im, *Nat. Mater.* **2017**, *16*, 543–550.